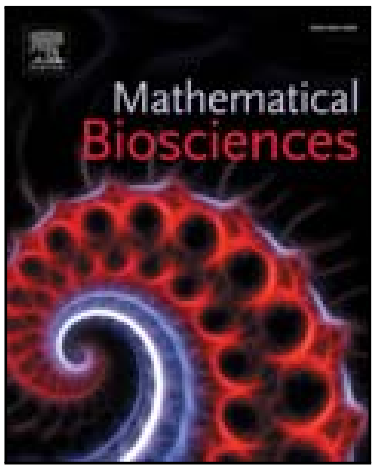

Random migration processes between two stochastic epidemic centers

Igor Sazonov, Mark Kelbert, Michael B. Gravenor

PII: S0025-5564(16)00022-5
DOI: 10.1016/j.mbs.2016.01.011
Reference: MBS 7746

To appear in: *Mathematical Biosciences*

Received date: 12 August 2015
Revised date: 19 January 2016
Accepted date: 28 January 2016

Please cite this article as: Igor Sazonov, Mark Kelbert, Michael B. Gravenor, Random migration processes between two stochastic epidemic centers, *Mathematical Biosciences* (2016), doi: 10.1016/j.mbs.2016.01.011

Highlights

- A simplest network of two stochastic epidemic centers coupled by a random migration is modelled.
- The interaction between susceptible/infected/removed individuals as well as their migration is described by a Markov chain.
- The mean field dynamics shows that the host and guest species should be accounted separately.
- It is shown that the small initial contagion (SIC) approximation (being much faster in terms of the CPU time than the direct numerical simulation) gives a good estimates for the mean value and the standard deviation of number of infective individuals.

Random migration processes between two stochastic epidemic centers

Igor Sazonov

Swansea University, Bay Campus, Fabian Way, SA1 8EN, U.K.

Mark Kelbert

National Research University Higher School of Economics, Moscow, R.F., Swansea University, Singleton Park, Swansea, SA2 8PP, U.K.

Michael B. Gravenor

Swansea University, Singleton Park, Swansea, SA2 8PP, U.K.

Abstract

We consider the epidemic dynamics in stochastic interacting population centers coupled by a random migration. Both the epidemic and the migration processes are modelled by Markov chains. We derive explicit formulae for the probability distribution of the migration process, and explore the dependence of outbreak patterns on initial parameters, population sizes and coupling parameters, using analytical and numerical methods. The mean field approximation for a general migration process is derived and an approximate method that allows the computation of statistical moments for networks with highly populated centers is proposed and tested numerically.

Keywords: epidemic modelling, population dynamics, Markov chains,

Email addresses: i.sazonov@swansea.ac.uk (Igor Sazonov), m.kelbert@swansea.ac.uk (Mark Kelbert), m.b.gravenor@swansea.ac.uk (Michael B. Gravenor)

stochastic processes, network interactions

Introduction

An epidemic outbreak of an infectious disease in a single population or in a network of populated centers develops stochastically due to random interactions between discrete individuals, both within a population center and due to a random migration between centers that make up a network. Conventionally, an outbreak in a highly populated center can be described by a simplified deterministic processes in accordance with the Law of Large Numbers (LLN) [1]. In this manner, the mean field approximation (hydrodynamic limits) of the appropriate statistical models will establish the basic relationship between the stochastic processes and the deterministic dynamical equations, for example the classic SIR model (susceptible/infected/ removed) and its large family (SEIR, SIS, MSIR, etc.)

However, there are important cases when stochastic effects are essential. Firstly, it is obviously important when the populations in centers are not large. The second less obvious scenario can occur at the initial stage of outbreak when the number of infectives is small. At this stage, the discreteness of the population can essentially affect the dynamics of the outbreak. For an isolated center, these effects have been thoroughly studied, for example in [2]. A proper analysis of a network of interacting epidemic centers requires an account of the stochastic migration fluxes between them.

If the initial number of infectives triggering the outbreak in a particular populated center is small (as is typical) then the LLN fails at least for the initial time period until the number of infectives is large enough. For this

reason the observed number of infectives can, at times, be significantly different from the prediction of a deterministic model, i.e. the standard deviation of the number of infectives, and, consequently, of the time until the peak outbreak can be wide even in a highly populated center or a network of such centers.

In principle, the probability density function (PDF), its standard deviation, and other important characteristics for the outbreak forecast could be determined by a direct numerical simulation. However, this simulation will tend to be computationally costly. Here, our goal is to develop a technique for an analytical estimation of the outbreak statistical characteristics by applying some perturbation methods.

Our toolkit is the so-called small initial contagion (SIC) approximation, relevant for the case of a large populated center over the period in which the initial number of infectives is small, cf. [2]. For a network of highly populated SIR centers, and in the framework of deterministic models, the technique is described in [3, 4]. In this paper, we develop a stochastic version of the SIC approach, based on the assumption that in the real epidemic centers the number of infectives triggering an outbreak is still small. In these situations, our proposed SIC approach acts as a key to solving the properties of cumbersome epidemic networks. In this work we consider the simplest network in which the migration process is already essential: two stochastic SIR centers coupled by random migration between them. This gives us opportunity to focus on the effect of migration. More general networks will be considered in subsequent works.

We have previously considered a stochastic analogue of the standard SIR

model [2]. Using the SIC approximation, one can distinguish two linked stages of epidemic evolution. At stage 1, of initial contamination, the number of infectives is small and a discrete formulation is vital. At this stage the system is random, and governed by stochastic equations. At stage 2, the developed outbreak, the numbers of individuals in all the components are large, hence the LLN is appropriate and the standard deterministic SIR model can describe the outbreak process accurately enough (with the benefits of its simple sets of equations). Putting these two stages together, it is therefore natural to consider a deterministic system for any particular outbreak, but with random initial conditions that are provided by the output from the stochastic stage 1. The statistical characteristics of the complete model are then obtained by applying the deterministic equations with random initial conditions using the matching asymptotic expansions technique (cf. [5]). In contrast to the traditional technique, the asymptotic approximation of a stochastic system (at a brief initial period) is matched with a deterministic evolution with random initial conditions (for all other times). Nevertheless, as in the traditional approach, we match the approximations at some intermediate time t_* in the interval where both approximations are valid (cf. [5]).

The Markov chain (MC) describing the stochastic SIR model has been studied previously, e.g., in [6] where a partial differential equation (PDE) for the moment generating function was derived.

The stochastic SIR model admits a number of generalizations and extensions, see e.g. [7, 8, 9, 10]. An analogous technique has also been applied for the stochastic SIS model in [11]. Here, we develop a similar approach

for a pair of linked centers and obtain approximate formulae for their main statistical characteristics. We show that the results of large-scale numerical simulation are in a good agreement with the appropriately estimated analytical models.

This paper is organized as follows. In Section 1 we introduce a Markov chain model describing a random epidemic outbreak in two populated centers coupled by a random process of migration of all types of population individuals. In this section we establish the convergence of this model to the deterministic mean-field model proposed in [12], though some technical details are presented in the Appendix. In Section 2 we describe a model of random migration between two interacting SIR centers taking place before the outbreak to determine all the initial conditions for the Markov chain. model. In this process, migration between centers is also modelled by a Markov chain. We derive the Master/Kolmogorov equations for the probability generating functions (PGF) and solve them analytically. This analysis confirms the diffusion-like model of migration heuristically proposed in [12]. In Section 3 the numerical algorithm for directly solving the Markov chain model is described, the dependence of outbreak characteristics on the population size, the initial number of infectives and the migration parameters are presented and discussed. In Section 4 a two-stage semi-random model is investigated both analytically and numerically. Finally, in Discussion we make some comparisons with previously considered models and outline the prospects for future development.

1. Stochastic model of two SIR centers interaction

Continuous-time Markov chain (MC) models are of vital importance to mathematical epidemiology because they capture the stochastic nature of individual-to-individual disease transmission [7, 8, 9, 10, 11]. For this reason they are particular relevant on the early and final stages of epidemic when the number of new cases is not particular large. On the stage of developed epidemic the LLN provides a deterministic approximation in a large enough population. Kurtz [13] and Barbour [14] justified this fluid (or hydrodynamical) approximation rigorously for a suitably scaled version of the process and studied the diffusion approximation for the scaled fluctuations around the hydrodynamical limits. We adopt their technique for a model of interaction centers described below.

Consider two populated centers, or nodes, 1 and 2, with initial populations N_1 and N_2, respectively. Let $S_n(t)$, $I_n(t)$, $R_n(t)$ be the numbers of (resident) host susceptibles, infectives and removed, respectively, in node n at time t. Let $S_{mn}(t)$, $I_{mn}(t)$, $R_{mn}(t)$ be numbers of guest susceptibles, infectives and removed, respectively, in node n migrated (visiting) from node m at time t. Note that in the standard SIR model, removed individuals do not interact with others, and hence do not affect the dynamics of susceptibles or infectives, and can be omitted from consideration [6, 15, 16].

Assume that the populations in every node are completely mixed, and the contamination rate β_n of a susceptible individual in node n at time interval $[t, t + \mathrm{d}t]$ is proportional to the number of all infectives in node n: that is host (resident) infectives I_n at time t plus guest infectives I_{mn} migrated from node m. Next, every infective in node n can be removed (representing, for

example, recovery) with probability rate α_n (cf. [2]).

The model now requires a migration rate γ_{nm} from node n to node m and return rate δ_{mn} for a guest individual to return to his resident home node, they may be different for different populations, i.e., we specify the migration process for susceptibles by parameters γ^S_{nm},δ^S_{mn} and for infectives—γ^I_{nm},δ^I_{mn} (cf. [12]). In reality, the return rate to the host node should usually be higher than the migration rate to a neighbouring node, i.e., $\gamma^I_{mn} < \delta^I_{nm}$, $\gamma^S_{mn} < \delta^S_{nm}$.

Taking into account the above specifications, we model a network of two SIR centers interacting due to migration of individuals between them by a Markov chain (MC), with a full description as summarized in Table 1.

In this model we assume the total number of individuals in the both centers to be constant $N_1 + N_2$. Also the number of every species (host and migrated) cannot exceed N_1 or N_2 in the node 1 and 2, respectively. This gives us the restriction presented in Table 1.

If I_0 infectives appear in center 1 at time $t = 0$ then the initial conditions take the form

$$\begin{aligned} &I_1 = I_0,\ S_1 = N_1 - I_0 - S^0_{12},\ I_{12} = 0,\ S_{12} = S^0_{12}, \\ &I_2 = 0,\ \ S_2 = N_2 - S^0_{21}, \qquad\quad I_{21} = 0,\ S_{21} = S^0_{21}. \end{aligned} \tag{1}$$

Here, the initial numbers of guest susceptibles S^0_{12} and S^0_{21} are random and determined by migration processes between centers taking place before the appearance of a single infective. In Section 2 we determine this distribution (which turns out to be binomial) by considering the pure migration processes that take place before the outbreak: see Eq. (19) below. Mean values for S^0_{12} and S^0_{21} are given by (9).

Numerical simulations based on this model are presented and discussed

Table 1: Markov's chain for two coupled SIR nodes

i	Process $\#i$	Rate, ν_i	Restriction	Description
1	$S_1 \to S_1 - 1$ $I_1 \to I_1 + 1$	$\beta_1(I_1+I_{21})S_1$	$I_1 \leq N_1$	Contamination in 1 (host)
2	$S_{21} \to S_{21} - 1$ $I_{21} \to I_{21} + 1$	$\beta_1(I_1+I_{21})S_{21}$	$I_{21} < N_2$	Contamination in 1 (guest)
3	$I_1 \to I_1 - 1$	$\alpha_1 I_1$		Recovering in 1 (host)
4	$I_{21} \to I_{21} - 1$	$\alpha_1 I_{21}$		Recovering in 1 (guest)
5	$S_1 \to S_1 - 1$ $S_{12} \to S_{12} + 1$	$\gamma^S_{12} S_1$	$S_{12} \leq N_1$	Migration from 1 to 2
6	$I_1 \to I_1 - 1$ $I_{12} \to I_{12} + 1$	$\gamma^I_{12} I_1$	$I_{12} \leq N_1$	Migration from 1 to 2
7	$S_1 \to S_1 + 1$ $S_{12} \to S_{12} - 1$	$\delta^S_{21} S_{12}$	$S_1 \leq N_1$	Return from 2 to 1
8	$I_1 \to I_1 + 1$ $I_{12} \to I_{12} - 1$	$\delta^I_{21} I_{12}$	$I_1 \leq N_1$	Return from 2 to 1
9	$S_2 \to S_2 - 1$ $I_2 \to I_2 + 1$	$\beta_2(I_2+I_{12})S_2$	$I_2 \leq N_2$	Contamination in 2 (host)
10	$S_{12} \to S_{12} - 1$ $I_{12} \to I_{12} + 1$	$\beta_2(I_2+I_{12})S_{12}$	$I_{12} \leq N_1$	Contamination in 2 (guest)
11	$I_2 \to I_2 - 1$	$\alpha_2 I_2$		Recovering in 2 (host)
12	$I_{12} \to I_{12} - 1$	$\alpha_2 I_{12}$		Recovering in 2 (guest)
13	$S_2 \to S_2 - 1$ $S_{21} \to S_{21} + 1$	$\gamma^S_{21} S_2$	$S_{21} \leq N_2$	Migration from 2 to 1
14	$I_2 \to I_2 - 1$ $I_{21} \to I_{21} + 1$	$\gamma^I_{21} I_2$	$I_{21} \leq N_2$	Migration from 2 to 1
15	$S_2 \to S_2 + 1$ $S_{21} \to S_{21} - 1$	$\delta^S_{12} S_{21}$	$S_2 \leq N_2$	Return from 1 to 2
16	$I_2 \to I_2 + 1$ $I_{21} \to I_{21} - 1$	$\delta^I_{12} I_{21}$	$I_2 \leq N_2$	Return from 1 to 2

in Section 3. Since an analytical approach taken via the Master/Kolmogorov equations (see [13]) is cumbersome, having a complicated analysis and solution for the general case, our aim here is to develop reasonable approximations.

It is well-known that a pure jump Markov process converges to a solution of differential equation in the so-called fluid or mean-field limit, see [13, 17]. This general approach adopted for a vector process defined in Table 1 is presented below.

Proposition 1. Consider a Markov chain (MC) $\{I_n(t), S_n(t), I_{nm}(t), S_{nm}(t)\}$ defined in Table 1 and subject to initial conditions (1). Introducing a large parameter Λ consider also the scaled MC $\{I_n^*(t), S_n^*(t), I_{nm}^*(t), S_{nm}^*(t)\}$ $(n = 1, 2,\ m = 2, 1)$

$$\begin{aligned} I_n^*(t) &= \Lambda^{-1} I_n(t), \quad S_n^*(t) = \Lambda^{-1} S_n(t), \\ I_{nm}^*(t) &= \Lambda^{-1} I_{nm}(t), \quad S_{nm}^*(t) = \Lambda^{-1} S_{nm}(t) \end{aligned} \tag{2}$$

in populations of sizes $\Lambda N_n, \Lambda N_m$ obtained by scaling the transition rates $\beta_n \to \Lambda^{-1}\beta_n$, and scaling of initial conditions as

$$\begin{aligned} I_1(0) &= \Lambda I_0, \quad S_1(0) = \Lambda(N_1 - I_0 - S_{12}^0), \\ I_2(0) &= 0, \qquad S_2(0) = \Lambda\left(N_2 - S_{21}^0\right), \\ I_{12}(0) &= 0, \qquad S_{12} = \Lambda S_{12}^0, \\ I_{21}(0) &= 0, \qquad S_{21} = \Lambda S_{21}^0 \end{aligned} \tag{3}$$

where independent random variables S_{12}^0 and S_{21}^0 have binomial PDFs (19). The scaled MC converges in distribution as $\Lambda \to \infty$ to the deterministic

functions $\{\hat{I}_n(t),\, \hat{S}_n(t),\, \hat{I}_{nm}(t),\, \hat{S}_{nm}(t)\}$ satisfying the following ODEs

$$\frac{\mathrm{d}}{\mathrm{d}t}\hat{S}_n = -\beta_n \hat{S}_n(\hat{I}_n + \hat{I}_{mn}) - \gamma^S_{nm}\hat{S}_n + \delta^S_{mn}\hat{S}_{nm} \tag{4}$$

$$\frac{\mathrm{d}}{\mathrm{d}t}\hat{I}_n = \beta_n \hat{S}_n(\hat{I}_n + \hat{I}_{mn}) - \alpha_n \hat{I}_n - \gamma^I_{nm}\hat{I}_n + \delta^I_{mn}\hat{I}_{nm} \tag{5}$$

$$\frac{\mathrm{d}}{\mathrm{d}t}\hat{S}_{mn} = -\beta_n \hat{S}_{mn}(\hat{I}_n + \hat{I}_{mn}) + \gamma^S_{mn}\hat{S}_m - \delta^S_{nm}\hat{S}_{mn} \tag{6}$$

$$\frac{\mathrm{d}}{\mathrm{d}t}\hat{I}_{mn} = \beta_n \hat{S}_{mn}(\hat{I}_n + \hat{I}_{mn}) - \alpha \hat{I}_{mn} + \gamma^I_{mn}\hat{I}_m - \delta^I_{nm}\hat{I}_{mn} \tag{7}$$

(cf. [12]), and subject to the initial conditions

$$\begin{aligned} \hat{I}_1(0) &= I_0, \quad \hat{S}_1(0) = N_1 - I_0 - \bar{S}^0_{12}, \\ \hat{I}_2(0) &= 0, \quad \hat{S}_2(0) = N_2 - \bar{S}^0_{21}, \\ \hat{I}_{12}(0) &= 0, \qquad \hat{S}_{12} = \bar{S}^0_{12}, \\ \hat{I}_{21}(0) &= 0, \qquad \hat{S}_{21} = \bar{S}^0_{21} \end{aligned} \tag{8}$$

where

$$\bar{S}^0_{12} = \frac{\gamma^S_{12}N_1}{\gamma^S_{12} + \delta^S_{21}}, \quad \bar{S}^0_{21} = \frac{\gamma^S_{21}N_2}{\gamma^S_{21} + \delta^S_{12}}. \tag{9}$$

In fact, equations (4)–(7) can be derived phenomenologically: if the number of individuals is large enough, its change by one or by a few can be considered as infinitesimally small. For example, the number of infectives I_1 can increase due to process #1 and #8 with rates $\beta_1(I_1{+}I_{21})S_1$ and $\delta^I_{21}I_{12}$, respectively, or decrease due to process #3 and #6 with rates $\alpha_1 I_1$ and $\gamma^I_{12}I_1$, respectively. Therefore the rate of $\mathrm{d}I_1$ in time interval $\mathrm{d}t$ can be estimated as $\mathrm{d}I_1 = \big[\beta_1(I_1{+}I_{21})S_1 + \delta^I_{21}I_{12}\big]\mathrm{d}t - \big[\alpha_1 I_1 + \gamma^I_{12}I_1\big]\mathrm{d}t$, that gives Eq. (5) for $n = 1, m = 2$. The same holds for all other individuals. This argument can be made rigorous with the help of Law of Large Numbers (LLN). This, then, indicates that the mean values of the variables converge to the mean-field (hydrodynamic) limit.

The more delicate question is to establish the convergence in probability. The formal mathematical proof neatly follows the papers [13, 17] where the setting is slightly different. See Appendix for the sketch of additional arguments.

2. Random migration of non-contaminating individuals

In order to elaborate the distributions for S^0_{nm} existing at the very beginning of the outbreak we study the pure migration process, setting $I_1 \equiv 0, I_2 \equiv 0$. In this case, the MC described in Table 1 can be split into two independent processes: $S_1 \leftrightarrow S_{12} = N_1 - S_1$, and $S_2 \leftrightarrow S_{21} = N_2 - S_2$. For each of them we have the following MC in terms of a single random variable S_n, $n = 1, 2$:

Process	Rate
$S_n \to S_n - 1$	$\gamma^S_{nm} S_n$
$S_n \to S_n + 1$	$\delta^S_{mn}(N_n - S_n)$

(10)

Introduce the notation

$$\lceil k \rceil_0^N = \begin{cases} k, & 0 \le k \le N \\ 0, & \text{otherwise.} \end{cases} \tag{11}$$

Let $P_k(t) = \mathbb{P}(S_{nm}(t){=}k) \equiv \mathbb{P}(S_n(t){=}N_n - k)$ be the probability distribution in node m at instant t. Then the Master/Kolmogorov's equations take the form

$$\frac{\mathrm{d}}{\mathrm{d}t} P_k = \gamma \left(\lceil N - k + 1 \rceil_0^N \right) P_{k-1} - \gamma(N-k) P_k + \delta \left(\lceil k + 1 \rceil_0^N \right) P_{k+1} - \delta k P_k \tag{12}$$

where $0 \le k \le N$; for the sake of simplicity we temporary set $\gamma = \gamma^S_{nm}$, $\delta = \delta^S_{mn}$, $N = N_n$. Notation (11) makes enable us to write the equations for $k = 0$ and $k = N$ in the same form as the others.

For the probability generating function (PGF)

$$G(z,t) = \sum_{k=0}^{N} z^k P_k(t) \tag{13}$$

equations (12) implies the following PDE

$$\frac{\partial G}{\partial t} = (1-z)\left[(-\gamma z - \delta)\frac{\partial G}{\partial z} + \gamma N G\right]. \tag{14}$$

The initial condition $P_0(0) = 1, P_{k>1}(0) = 0$ implies

$$G(z,0) = 1. \tag{15}$$

The solution to problem (14)–(15) can be found explicitly

$$G(z,t) = \left[\frac{(\gamma z + \delta) - \gamma(z-1)e^{-(\gamma+\delta)t}}{\gamma+\delta}\right]^N. \tag{16}$$

Now one can calculate all the moments of distribution $\{P_k(t)\}$, say

$$\mathbb{E}S(t) \equiv \mu_1(t) = G_z(1,t) = N\varepsilon\left[1 - e^{-t/\tau}\right] \tag{17}$$

$$\mathrm{var}(S(t)) \equiv \mu_2(t) = G_{zz}(1,t) + \mu_1 - \mu_1^2 = \mu_1(t)\left[\varepsilon e^{-t/\tau} + (1-\varepsilon)\right] \tag{18}$$

where $\varepsilon = \gamma/(\gamma+\delta)$, $\tau = 1/(\gamma+\delta)$.

If the migration process has been operating for enough time before the outbreak starts, then the PGF takes its limiting form for $t \to \infty$

$$G(z,\infty) = (\varepsilon z + (1-\varepsilon))^N$$

which is the MGF for a binomial distribution:

$$\mathbb{P}(S^0_{nm} = k) = \binom{N_n}{k} \left(\varepsilon^S_{nm}\right)^k (1-\varepsilon^S_{nm})^{N_n - k}. \tag{19}$$

From here on we return to the indexed notation

$$\varepsilon_{nm}^{S,I} = \frac{\gamma_{nm}^{S,I}}{\gamma_{nm}^{S,I} + \delta_{mn}^{S,I}}. \tag{20}$$

This distribution has the following first two moments

$$\bar{S}_{nm}^0 \equiv \mathbb{E}S_{nm}^0 = \mu_1(\infty) = \varepsilon_{nm}^S N_n \tag{21}$$

$$\mathrm{var}(S_{nm}^0) = \mu_2(\infty) = N_n \varepsilon_{nm}^S (1 - \varepsilon_{nm}^S). \tag{22}$$

The relative standard deviation (i.e. for the process $X = S_{nm}/\bar{S}_{nm}^0$) decays as $N_n^{-1/2}$:

$$\sigma_{S_{nm}^0/\bar{S}_{nm}^0} = \frac{\sqrt{\mu_2(\infty)}}{\mu_1(\infty)} = \sqrt{\frac{1 - \varepsilon_{nm}^S}{\varepsilon_{nm}^S N_n}}. \tag{23}$$

Hence, when $N_n \to \infty$, the migration process tends in probability to the deterministic limit described in [12].

Thus, in the MC model defined in Table 1, the initial conditions S_{12}^0 and S_{21}^0 can be selected randomly from the binomial distribution (19) or approximated by a Gaussian function if N_n is large enough.

Parameter $\varepsilon_{nm}^S := \gamma_{nm}^S/(\gamma_{nm}^S + \delta_{nm}^S) = \bar{S}_{nm}^0/N_n$ indicates the mean share of individuals from node n migrated to node m. Obviously this share, on average, should be small for highly populated centers: considering a city for example, half the population cannot realistically be found to visiting another center for any reasonable period of time. Parameter ε_{nm}^S can be treated as a coupling parameter, that characterizes how intensive the migration fluxes are between populated centers. Analogous fluxes of infectives are considered unlikely to be more intensive, therefore $\varepsilon_{nm}^I = \gamma_{nm}^I/(\gamma_{nm}^I + \delta_{nm}^I) \leq \varepsilon_{nm}^S$. So, for highly populated centers, the following inequality holds

$$\varepsilon_{nm}^{S,I} \ll 1 \Longleftrightarrow \gamma_{mn}^{S,I} \ll \delta_{nm}^{S,I}. \tag{24}$$

The second important characteristic of the migration process is the characteristic migration time $\tau_{nm}^{S,I} = 1/(\gamma_{nm}^{S,I} + \delta_{nm}^{S,I})$. Eq. (17) implies that the dynamic equilibrium establishes after the migration process started or if the population changed suddenly at time $t = 0$, with a transitional time proportional to τ. Both pairs of parameters: $\{\gamma, \delta\}$ and $\{\varepsilon, \tau\}$ are uniquely related.

3. Direct numerical simulation of two interacting SIR centers

3.1. Numerical scheme

In the numerical simulation of the stochastic SIR model the time interval was divided into small steps Δt such that the sum of all rates from Table 1 multiplied by Δt is essentially less than 1:

$$\max_t \{\nu_\Sigma(t)\}\, \Delta t \ll 1 \Longrightarrow \Delta t = \min\{P_t/\nu_\Sigma(t)\} \tag{25}$$

where P_t is the admitted threshold, say, $P_t = 0.1$.

The probability that at least one event occurs in one unit of time is bounded by the sum of rates of all the processes $\nu_\Sigma(t) = \sum_{i=1}^{16} \nu_i$:

$$\begin{aligned}\nu_\Sigma(t) = {} & \beta_1 (I_1 + I_{21})\,(S_1 + S_{21}) + \beta_2\,(I_2 + I_{12})\,(S_2 + S_{12}) \\ & + \alpha_2(I_2 + I_{12}) + \alpha_1(I_1 + I_{21}) \\ & + \gamma_{12}^S S_1 + \gamma_{12}^I I_1 + \delta_{21}^S S_{12} + \delta_{21}^I I_{12} + \gamma_{21}^S S_2 + \gamma_{21}^I I_2 + \delta_{21}^S S_{12} + \delta_{12}^I I_{21}.\end{aligned}$$

In this relationship, we majorize $I_1, S_1 \le N_1$, $I_2, S_2 \le N_2$, $I_{12}, S_{12} \le N_1$,

$I_{21}, S_{21} \le N_2$, then

$$\begin{aligned}\max(\nu_\Sigma) = {} & (\beta_1+\beta_2)(N_1+N_2)^2 + (\alpha_1+\alpha_2)(N_1+N_2) \\ & + (\gamma_{12}^S + \gamma_{12}^I + \delta_{21}^I + \delta_{21}^S)N_1 + (\gamma_{21}^S + \gamma_{21}^I + \delta_{12}^I + \delta_{12}^S)N_2 \\ & + \gamma_{12}^S S_1 + \gamma_{12}^I I_1 + \delta_{21}^S S_{12} + \delta_{21}^I I_{12}.\end{aligned}$$

In fact, this value overestimates the realised total rate significantly, as it is very improbable that the numbers of guest susceptibles and infectives in a highly populated center exceeds the values $\varepsilon_{nm}^S N_n$ and $\varepsilon_{nm}^I N_n$, respectively, where $\varepsilon_{nm}^{S,I}$ is defined in (19), in virtue of (24). For this reason we can account that $S_{nm} \lesssim \varepsilon_{nm}^S N_n$ and $I_{nm} \lesssim \varepsilon_{nm}^I N_n$ (and also use the rigorous inequalities $I_n S_n \le \frac{1}{4}N_n^2$). Then we obtain the more realistic estimation:

$$\begin{aligned}\max(\nu_\Sigma) \simeq {} & \tfrac{1}{4}\beta_1 N_1^2 + \tfrac{1}{4}\beta_2 N_2^2 \\ & + \beta_1\left(\varepsilon_{21}^I + \varepsilon_{21}^S\right)N_2N_1 + \beta_2\left(\varepsilon_{12}^I + \varepsilon_{12}^S\right)N_2N_1 \\ & + \alpha_1\left(N_1 + \varepsilon_{21}^I N_2\right) + \alpha_2\left(N_2 + \varepsilon_{12}^I N_1\right) \\ & + \left(\gamma_{12}^S + \gamma_{12}^I\right)N_1 + \left(\varepsilon_{21}^S\delta_{12}^S + \varepsilon_{21}^I\delta_{12}^I\right)N_1 \\ & + \left(\gamma_{21}^S + \gamma_{21}^I\right)N_2 + \left(\varepsilon_{12}^S\delta_{21}^S + \varepsilon_{12}^I\delta_{21}^I\right)N_2 \\ & + \beta_1\varepsilon_{21}^I\varepsilon_{21}^S N_2N_1 + \beta_2\varepsilon_{12}^I\varepsilon_{12}^S N_2N_1.\end{aligned}$$

The following numerical scheme is used:

1. Assign the initial values to 8 variables

$$\begin{aligned}& I_1 = I_0,\ S_1 = N_1 - I_0 - S_{12}^0,\ I_{12} = 0,\ S_{12} = S_{12}^0, \\ & I_2 = 0,\ \ S_2 = N_2 - S_{21}^0, \qquad I_{21} = 0,\ S_{21} = S_{21}^0\end{aligned}$$

where S_{12}^0, S_{21}^0 are random numbers distributed in accordance with (19).

2. Calculate the current rates $\{\nu_i, i = 1, \ldots, 16\}$ indicated in Table 1.
3. Calculate the current probability of at least one event occurrence in accordance with eq. (25):

$$p = \Delta t\, \nu_\Sigma(t) \equiv \Delta t \sum_{i=1}^{16} \nu_i.$$

4. Generate uniformly distributed random number $x \in [0, 1]$.
5. If $x > p$ then no events occur. In this case:
   (a) advance one step in time: $t \leftarrow t + \Delta t$ without changing variables $I_1, \ldots, S_{21}$, also $\nu_1, \ldots, \nu_{16}$ and p;
   (b) if $t > t_{\max}$ terminate the process, otherwise go to step 4.

   If $x \leq p$ then at least one event occurs. In this case:
   (a) calculate the intervals $\Delta y_i = [\eta_{i-1}, \eta_i]$, $\eta_i = \sum_{j=1}^{i} \nu_j$;
   (b) generate the second random number y uniformly distributed in $[0, \eta_{16}]$;
   (c) find in which interval y falls;
   (d) perform the process described in Table 1 with the correspondent rate;
   (e) advance one step in time: $t \leftarrow t + \Delta t$;
   (f) if $t > t_{\max}$ terminate the process, otherwise go to step 2.

3.2. Numerical results

For numerical computation a basic model with two identical centers has parameters: $N_{1,2} = 10^4$, $\alpha_{1,2} = 1$, $R_{01,2} = 4$, $\varepsilon_{1,2}^{I,S} = 0.01$, $\tau_{1,2}^{I,S} = 5$ where $R_{01,2} = (\beta_{1,2}/\alpha_{1,2})\, N_{1,2}$ are the basic reproduction numbers for every center

[16, 6]. The initial number of infectives in the first node $I_0 = i_0 N_1$ where $i_0 = 0.01$ is taken for the basic model.

A few realizations of numerical computation are depicted in Figure 1. Here the time dependence of the total number of infectives $I_n^\Sigma = I_n + I_{mn}$ in every node are shown and compared with the curves based on integration of the deterministic initial value problem (4)–(9).

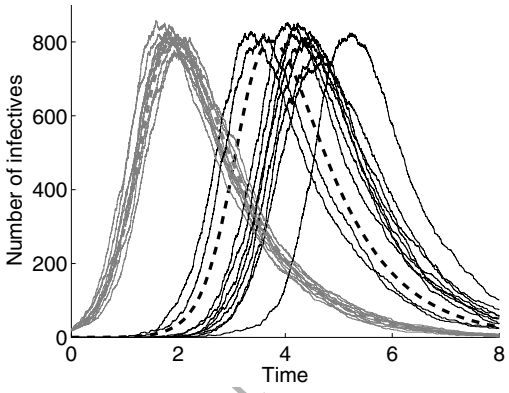

Figure 1: Examples of realizations of two stochastic SIR models. The total number of infectives is plotted in node 1 ($I_1^\Sigma = I_1 + I_{21}$) by thin grey lines and in node 2 ($I_2^\Sigma = I_2 + I_{12}$) by thin black lines. Bold dashed lines indicates the hydrodynamic limit. ($N_1 = N_2 = 2$k, $\mathrm{Ro}_1 = \mathrm{Ro}_2 = 4$, $\varepsilon = 0.01$, $\tau = 5$, $I_0/N_1 = 0.01$).

In the first set of numerical experiments, the total population size varies from $N_1 = N_2 = N = 400$ up to 10^6. In general, the number of realizations L was taken $L = 10^4$ but L was selected greater for small populations $N = 400$ and 2000 and smaller for extremely high populations: 250k and 1000k. The current mean number of total infectives $\overline{I}_{1,2}^\Sigma(t)$ and standard deviation are computed. The results of the first set are shown in Figure 2. Observe that the mean value of the random process (solid lines) converges to the solution

of the correspondent deterministic problem (bold dashed lines). But the convergence is much slower for node 2: for $N_1 = 10$k the mean trajectory practically coincides with the deterministic limit, on the other side the same effect in node 2 requires $N_{21} \sim 250$k.

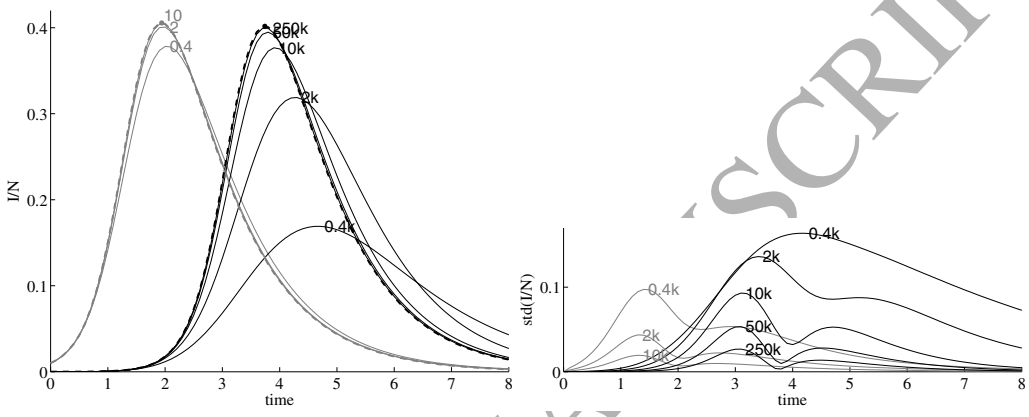

Figure 2: Evolution of the mean values for I_m^Σ/N_m $m = 1, 2$ (left) and their standard deviations (right). Grey curves for node 1, black lines for node 2. Dashed lines indicate the hydrodynamic limit described by eqs. (4)–(7). The node population is indicated near the top of the correspondent curve.

The convergence rate is examined in Figure 3. One can see that for node 1 the convergence rate almost coincides with $O(N^{-1/2})$, as for node 2 the decay rate tends to $O(N^{-1/2})$ only for sufficiently large population: $N = 10^6$. Thus, for the secondary contaminated node, taking into account the stochastic nature of the process is essential even if its population is large, provided that the migration parameters $\varepsilon_{1,2}^{I,S}$ are small (0.01 in this case). Say, if $N_2 = 400$ the standard deviation exceeds the mean value, for all times up to the peak outbreak.

In the second set of numerical experiments, we study the dependence of

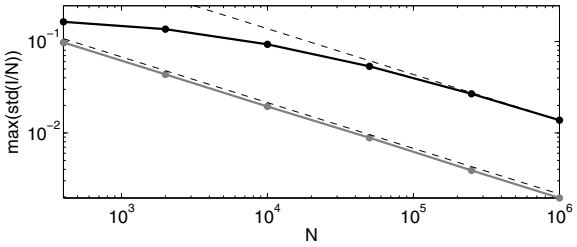

Figure 3: Maximal value of the standard deviation for processes I_1/N_1 and I_2/N_2 vs population $N = N_1 = N_2$. Black curves for node 1, grey lines for node 2. The slope of dashed line corresponds to the decay law $N^{-1/2}$.

the mean number of infectives and their standard deviation from the initial number of infectives I_0 in node 1, varying from 1 to 100 (the share $i_0 = I_0/N_1$ varies from 10^{-4} to 10^{-2}). The results are plotted in Figure 4. Because the time to the peak outbreak depends on the initial number of infectives, the mean-field curves become quite different. Therefore it is appropriate to shift the time so that the peak outbreaks for different initial conditions are at the same instant, say, $t = 0$. Then all the curves are very close to each other and practically coincide with the curve for the limiting solution introduced in [3, 4]. Observe that the smaller the number of initial infectives, the greater is the standard deviation (std) and the larger is the difference between the mean curve for the random process and the mean-field curve. Also observe that for node 1, the discrepancy of mean number of infectives from the mean-field limit, as well as the standard deviation, monotonically decay with the growth of I_0. In node 2 the analogous discrepancy and the std slightly change when the number of initial infective varies from 10 to 100.

In the third set of numerical experiments we study dependence of the mean number of infectives on the coupling coefficient ε (the same for all

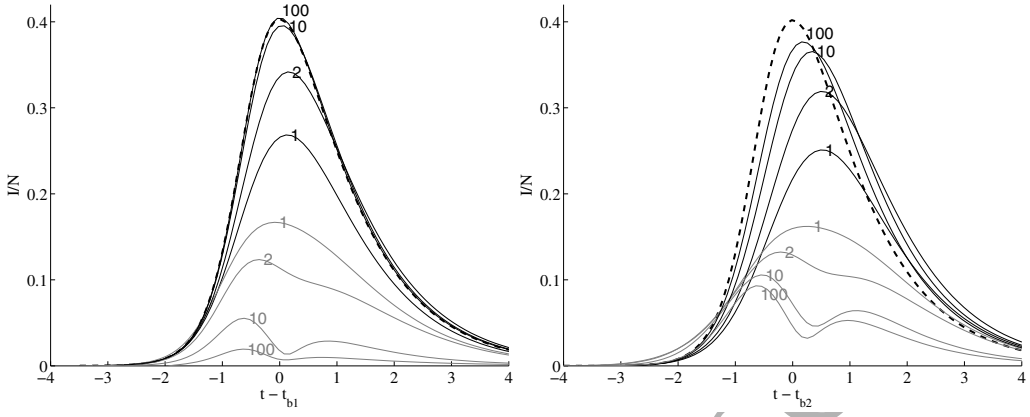

Figure 4: Left: Mean values for I_1^Σ/N_1 (black) and its standard deviation stdI_1^Σ/N_1 (grey) for different I_0. The initial number of infectives in node 1 is indicated near the top of the corresponding curve. Dashed line indicates the deterministic limiting solution. Right: the same for I_2^Σ/N_2.

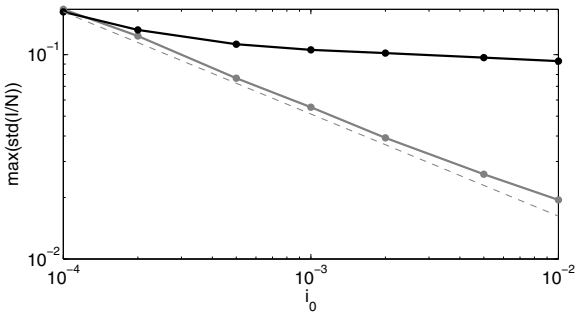

Figure 5: Maximal value of the standard deviation for I_1/N_1 and I_2/N_2 process vs population I_0 Grey curve is for node 1, black curve is for node 2. The dashed line has the slope corresponding to the decay law $N^{-1/2}$.

species). It was varied in the range $10^{-4}, ..., 10^{-1}$. The results are plotted in Figures 6 and 7. Observe that ε practically does not affect the standard deviation of the total number of infectives in node 1. The discrepancy of the mean curve from the mean-field curve becomes noticeable only for small ε:

$\varepsilon \lesssim 0.05$.

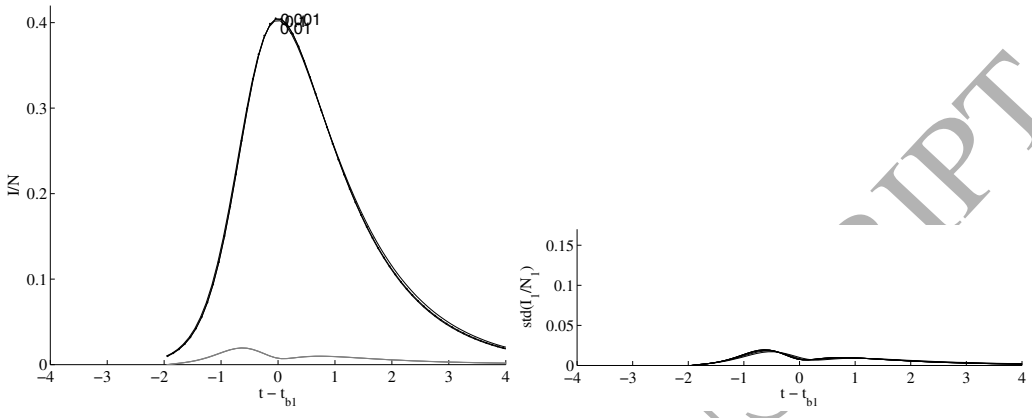

Figure 6: Mean values for I_1^Σ/N_1 (left) and its standard deviations $\mathrm{std}I_1^\Sigma/N_1$ (right) for different migration coefficient ε. Dashed lines indicate the mean-field limit. The initial number of infectives in node 1 is indicated near the top of the corresponding curve.

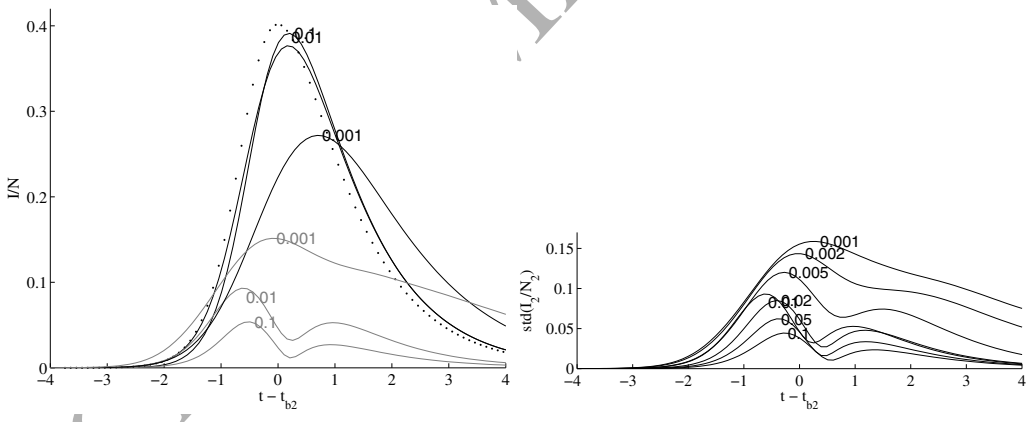

Figure 7: Mean values for I_2^Σ/N_2 (left) and its standard deviations $\mathrm{std}I_2^\Sigma/N_2$ (right) for different migration coefficient ε. Dashed lines indicate the mean-field limit. The initial number of infectives in node 1 is indicated near the top of the corresponding curve.

As for the second node, the standard deviation grows monotonically with a decrease in the coupling. That indicates the importance of accounting for

the random elements of the epidemic process in the case of weak coupling (i.e. in the case of relatively slow migration fluxes).

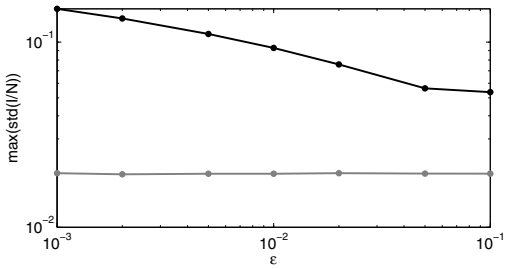

Figure 8: Maximal value of the standard deviation for processes I_1/N_1 and I_2/N_2 vs population $N = N_1 = N_2$. Grey curve is for node 1, black curve is for node 2. The dashed line has the slope corresponding to the decay law $N^{-1/2}$.

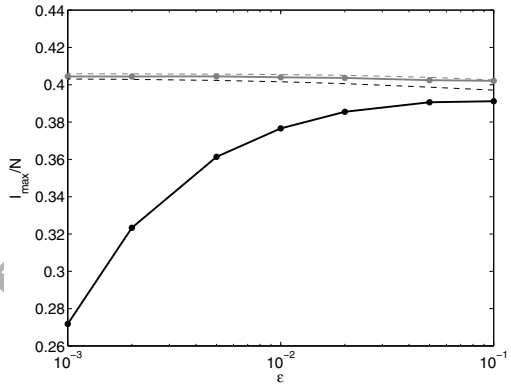

Figure 9: Outbreak value for I_1/N_1 and I_2/N_2 processes vs population $N = N_1 = N_2$ Grey curve is for node 1, black curve is for node 2. The dashed line are for the mean-field values.

Table 2: MC model for a general network of interacting centers ($m, n = 1, ..., M, m \neq n$)

Process	Rate
$S_n \to S_n{-}1, I_n \to I_n{+}1$	$\beta_n(I_n{+}\sum_m I_{mn})S_n$
$S_{mn} \to S_{mn}{-}1, I_{mn} \to I_{mn}{+}1$	$\beta_n(I_n{+}\sum_m I_{mn})S_{mn}$
$I_n \to I_n{-}1$	$\alpha_n I_n$
$I_{mn} \to I_{mn}{-}1$	$\alpha_n I_{mn}$
$S_n \to S_n{-}1, S_{nm} \to S_{nm}{+}1$	$\gamma^S_{nm} S_n$
$I_n \to I_n{-}1, I_{nm} \to I_{nm}{+}1$	$\gamma^I_{nm} I_n$
$S_n \to S_n{+}1, S_{nm} \to S_{nm}{-}1$	$\delta^S_{mn} S_{nm}$
$I_n \to I_n{+}1, I_{nm} \to I_{nm} - 1$	$\delta^I_{mn} I_{nm}$

4. Two-stage semi-random model

The MC model for two coupled SIR centers can be readily generalized for an arbitrary network of M mutually interacting SIR centers as described in Table 2.

In general, to study migration fluxes ($\gamma^{S,I}_{nm}, \delta^{S,I}_{mn} > 0$) between every pair of centers (of different rates) we have to consider $2M$ host and $2M(M-1)$ guest individuals. The correspondent MC model will contain $4M^2$ fluxes. The total rate can be evaluated via $\nu_\Sigma = O(M^2N^2)$. Therefore for a network containing a significant number of highly populated centers (say, main cities within a country), the time interval Δt will have to be taken extremely small, and, hence, the CPU time for a single realization will be considerable, and obtaining statistical properties across many realisations will be impractial. Thus the MC requires an accurate simplification to proceed with numerical modelling.

4.1. The small initial contagion (SIC) approximation

The SIC approximation is based on the assumptions which appear relevant for application in a network of highly populated centers:

- Population in every center is high: $N_n \gg 1$.
- Migration fluxes between the centers are small: $\varepsilon_{nm}^{S,I} \ll 1$.
- Initial number of infectives in the first contaminated center (say, $n = 1$), is small: $I_0 \ll N_1$.
- Reproduction number exceeds unity and is not very close to it in all the nodes: $R_{0n} := \beta_n N_n/\alpha_n > 1 + r$ where $r = O(1), r > 0$.

Using these assumptions, the outbreak process in every center can be split into the following main stages:

1. **Contaminating stage**: the number of infectives is small $I_n \ll N_n, S_n \approx N_n$ and the fluxes of infectives caused by migration are essential for the outbreak process (excepting the first node).
2. **Developed outbreak**: $I_n \gg 1$, when the contribution of migration fluxes is negligible (also the mean-field description for every individual realization is adequate).
3. **Recovering stage**: the node is not affected by infective immigrants and does not significantly affect contamination of other nodes.

It follows from these assumptions that the outbreak dynamics in the first node can be considered independently, and can be described by the following

MC

Process	Rate
$S_1 \to S_1{-}1, I_1 \to I_1{+}1$	$\beta_1 S_1 I_1$
$I_1 \to I_1{-}1$	$\alpha_1 I_1$

(26)

with the initial condition $I_1(0) = I_0$, $S_1 = N_1 - I_0$ studied in [6, 2]. At the contamination stage we have $S_1 \approx N_1$ and the MC can be further simplified

Process	Rate
$I_1 \to I_1{+}1$	$(\beta_1 N_1)\, I_1$
$I_1 \to I_1{-}1$	$\alpha_1 I_1$

(27)

The epidemic dynamics in node 2 at the contamination stage ($S_2 \approx N_2$) can be described by an analogous MC with an additional flux $\nu(t)$ of infectives migrated from node 1:

Process	Rate
$I_2 \to I_2{+}1$	$(\beta_2 N_2)\, I_2 + \nu(t)$
$I_2 \to I_2{-}1$	$\alpha_2 I_2$

(28)

with $I_2(0) = 0$ where

$$\nu(t) = (\beta_2 N_2) I_{12} + \delta_{12}^I I_{21}. \tag{29}$$

At the contamination stage, processes $I_{12}(t)$ and $I_{21}(t)$ are practically independent of process $I_2(t)$. Thus we have to consider MC (28) with a random flux $\nu(t)$, the statistical properties of which will be specified later.

4.2. Calculation of moments

First, we consider a single realization of the flux $\nu(t)$ and treat it as a deterministic function. Later we will use averaging on $\nu(t)$ to calculate the

moments of the distribution for $I_2(t)$.

4.2.1. Calculation of PGF $G(z,t)$ for a single realization

Let $P_k(t) = \mathbb{P}(I_2(t) = k)$ be the probability of k infectives I_2 at instant t. The initial condition is

$$P_0(0) = 1, \qquad P_{k>0}(0) = 0. \tag{30}$$

Kolmogorov's equations for MC (28) are

$$\tfrac{\mathrm{d}}{\mathrm{d}t}P_k = \beta_2'(\lceil k-1 \rceil_0^{N_2})P_{k-1} - \beta_2' k P_k + \alpha_2(\lceil k+1 \rceil_0^{N_2})P_{k+1} - \alpha_2 k P_k + \nu P_{k-1} - \nu P_k. \tag{31}$$

Here $\beta_2' = \beta_2 N_2$. For the PGF $G(z,t)$ tending $N_2 \to \infty$ (with $\beta_2 \to 0$, $\beta_2' = const$) we obtain the following PDE

$$\frac{\partial G}{\partial t} = (z-1)\left[(\beta_2' z - \alpha_2)\,\frac{\partial G}{\partial z} + \nu(t) G\right] \tag{32}$$

with the initial condition $G(z,0) = 1$. Its solution can be written in the integral form

$$G(z,t) = \exp\Big\{ - \int_0^t \frac{\lambda_2(z-1)\,\nu\,(t')\;\mathrm{d}t'}{\beta_2'(z-1) - (\beta_2' z - \alpha_2)\,e^{\lambda_2(t'-t)}} \Big\} \tag{33}$$

where $\lambda_2 = \beta_2' - \alpha_2 \equiv \alpha_2\,(R_{02}-1)$ is the initial growth rate of infectives in the deterministic SIR model in the limit $I_0/N \to 0$ (limiting solution introduced in [3, 4]).

4.2.2. Calculation of first moment $\mathbb{E}\,[I_2\,(t)]$

The first conditional moment $\mu_1(t\,|\,\nu) = \mathbb{E}(I_2(t)\,|\,\nu)$ for fixed $\nu(t)$ is

$$\mu_1(t\,|\,\nu) = G_z(1,t) = \int_0^t \nu\,(t')\,e^{\lambda_2(t-t')}\mathrm{d}t'. \tag{34}$$

Averaging over all realizations for $\nu(t)$ (with a time varying PDF $f_\nu(t)$): $\mu_1(t) = \mathbb{E}\mu_1(t\,|\,\nu)$

$$\mu_1(t) = \int \Big[\int_0^t f_\nu(t')\nu\,(t')\, e^{\lambda_2(t-t')} \mathrm{d}t' \Big] \mathrm{d}\nu = \int_0^t \bar{\nu}\,(t')\, e^{\lambda_2(t-t')} \mathrm{d}t' \tag{35}$$

where $\bar{\nu}(t) = \mathbb{E}\nu(t)$. Thus the average number of infectives in node 2 at the contamination stage relates with the flux $\nu(t)$ via the convolution

$$\mathbb{E}\left[I_2\,(t)\right] \equiv \mu_1\,(t) = \bar{\nu}\,(t) * e^{\lambda_2 t}. \tag{36}$$

4.2.3. Calculation of second moment $\mathrm{var}[I_2(t)]$

We apply the Law of Total Variation (e.g. [1]):

$$\mathrm{var}\left[I_2(t)\right] = \mathbb{E}\left[\mathrm{var}(I_2(t)\,|\,\nu)\right] + \mathrm{var}\left[\mathbb{E}(I_2(t)\,|\,\nu)\right]. \tag{37}$$

1. The first addend in (37) can be found through the PGF $G(z,t)$:

$$\begin{aligned} &\mathrm{var}(I_2(t)\,|\,\nu) = G_{zz}(1,t) + \mu_1(t\,|\,\nu) - \mu_1^2(t\,|\,\nu) \\ &= \frac{2\beta_2'}{\lambda_2} \int_0^t \nu(t') \left[e^{2\lambda_2(t-t')} - e^{\lambda_2(t-t')} \right] \mathrm{d}t' + \mu_1(t\,|\,\nu). \end{aligned}$$

After the averaging through ν we obtain

$$\mathbb{E}\left[\mathrm{var}(I_2(t)\,|\,\nu)\right] = \mu_1(t) + \frac{2\beta_2'}{\lambda_2} \int_0^t \bar{\nu}(t') \left[e^{2\lambda_2(t-t')} - e^{\lambda_2(t-t')} \right] \mathrm{d}t'.$$

Thus the first addend in (37) can be written as a sum of two convolutions

$$\mathbb{E}\left[\mathrm{var}(I_2(t)\,|\,\nu)\right] = \frac{2\beta_2'}{\lambda_2}\bar{\nu}(t) * e^{2\lambda_2 t} + (1 - \frac{2\beta_2'}{\lambda_2})\bar{\nu}(t) * e^{\lambda_2 t} \tag{38}$$

where $\bar{\nu}(t) = \beta_2'\bar{I}_{12}(t) + \delta_{12}^I \bar{I}_{21}(t)$.

2. To calculate the second addend in (37), we temporarily add μ_1^2 to it. Now it can be expressed via the covariance of flux $\nu(t)$:

$$\begin{aligned} &\mathrm{var}\left[\mathbb{E}(I_2(t)\,|\,\nu)\right] + \mu_1^2(t) = \mathbb{E}\left(\int_0^t \nu\,(t')\, e^{\lambda_2(t-t')} \mathrm{d}t' \right)^2 \\ &= \int_0^t \int_0^t \mathbb{E}\left[\nu\,(t')\,\nu\,(t'')\right] e^{\lambda_2(t-t')} \mathrm{d}t' e^{\lambda_2(t-t'')} \mathrm{d}t''. \end{aligned} \tag{39}$$

The function in the integrand can be represented as the sum

$$\mathbb{E}\left[\nu\left(t'\right)\nu\left(t''\right)\right] = \operatorname{cov}\left[\nu\left(t'\right),\nu\left(t''\right)\right] + \bar{\nu}(t')\bar{\nu}(t''). \tag{40}$$

Integration of the second addend in (40) gives just the temporary added term

$$\int_0^t \int_0^t \bar{\nu}(t')\bar{\nu}(t'')e^{\lambda_2(t-t')}\mathrm{d}t' e^{\lambda_2(t-t'')}\mathrm{d}t'' = \mu_1^2(t).$$

Thus the second addend in (37) can be written through the following integral

$$\operatorname{var}\left[\mathbb{E}\big(I_2(t) \mid \nu\big)\right] = \int_0^t \int_0^t \operatorname{cov}\left[\nu\left(t'\right),\nu\left(t''\right)\right] e^{\lambda_2(t-t')}\mathrm{d}t' e^{\lambda_2(t-t'')}\mathrm{d}t''. \tag{41}$$

in which we have to calculate the covariance of flux $\nu(t)$.

If flux $\nu(t)$ is a random process controlled by a MC, calculation of its covariance is a complicated task, and consideration of this is outside the scope of the present study. Remembering that the flux is a linear combination of two MC processes (29): $\nu(t) = \beta_2' I_{12}(t) + \delta_{12}^I I_{21}(t)$. Here we approximate $I_{12}(t)$ and $I_{21}(t)$ by two mutually independent Poisson processes with variable rates $\frac{\mathrm{d}}{\mathrm{d}t}\bar{I}_{12}(t)$ and $\frac{\mathrm{d}}{\mathrm{d}t}\bar{I}_{21}(t)$, respectively, where $\bar{I}_{12}(t)$ and $\bar{I}_{21}(t)$ are calculated below. In this approximation, using the independence of increments of the inhomogeneous Poisson flow (e.g. [18]) we can write

$$\begin{aligned}
&\operatorname{cov}\left[I_{12}\left(t'\right),I_{12}\left(t''\right)\right] \approx \bar{I}_{12}(\min\left\{t',t''\right\}),\\
&\operatorname{cov}\left[I_{21}\left(t'\right),I_{21}\left(t''\right)\right] \approx \bar{I}_{21}(\min\left\{t',t''\right\}),\\
&\operatorname{cov}\left[I_{12}\left(t'\right),I_{21}\left(t''\right)\right] \approx 0.
\end{aligned}$$

We justify this approximation numerically below. Thus, for the covariance of the flux we have

$$\operatorname{cov}\left[\nu\left(t'\right),\nu\left(t''\right)\right] = \varpi(\min\left\{t',t''\right\}), \quad \varpi(t) \equiv \left(\beta_2'\right)^2 \bar{I}_{12}(t) + \left(\delta_{12}^I\right)^2 \bar{I}_{21}(t). \tag{42}$$

Equation (42) holds true because the second central moment of the Poisson process coincides with the first moment. In this approximation, it is sufficient to compute the first moment of flux $\nu(t)$ in order to compute the second moment for I_2.

With the account for (42), we split integral (41) into two parts:

$$\begin{aligned}\operatorname{var}\left[\mathbb{E}\big(I_2(t) \mid \nu\big)\right] &\approx J_1 + J_2\\ J_1 &= \int_0^t \int_0^{t'} \varpi(t'') e^{\lambda_2(t-t'')} \mathrm{d}t'' e^{\lambda_2(t-t')} \mathrm{d}t'\\ J_2 &= \int_0^t \int_{t'}^t \varpi(t') e^{\lambda_2(t-t'')} \mathrm{d}t'' e^{\lambda_2(t-t')} \mathrm{d}t'.\end{aligned}$$

Integrating J_1 by parts and J_2 directly we find that they both give the same answer

$$J_1 = J_2 = \frac{1}{\lambda_2}\varpi(t) * e^{2\lambda_2 t} - \frac{1}{\lambda_2}\varpi(t) * e^{\lambda_2 t}.$$

Finally, combining the above results we have

$$\begin{aligned}\operatorname{var}(I_2) = {} & \frac{4\left(\beta_2'\right)^2}{\lambda_2} \bar{I}_{12} * e^{2\lambda_2 t} + \Big[\frac{2\beta_2'\delta_{12}^I}{\lambda_2} + \frac{2\left(\delta_{12}^I\right)^2}{\lambda_2}\Big] \bar{I}_{21} * e^{2\lambda_2 t}\\ & - \Big[\frac{4\left(\beta_2'\right)^2}{\lambda_2} - \beta_2'\Big] \bar{I}_{12} * e^{\lambda_2 t} - \Big[\frac{2\beta_2'\delta_{12}^I}{\lambda_2} + \frac{2\left(\delta_{12}^I\right)^2}{\lambda_2} - \delta_{12}^I\Big] \bar{I}_{21} * e^{\lambda_2 t}.\end{aligned} \tag{43}$$

4.2.4. Computation of the average flux $\bar{\nu}(t)$

It is natural to split the total flux into two parts $\nu(t) = \beta_2' I_{12} + \delta_{12}^I I_{21} = \nu_{12}(t) + \nu_{21}(t)$. Flux process $\nu_{12}(t)$ described by the MC

Process	Rate
$I_{12} \to I_{12}{+}1$	$\gamma_{12}^I I_1$
$I_{12} \to I_{12}{-}1$	$\left(\delta_{21}^I + \alpha_2\right) I_{12}$

(44)

(with $I_{12}(0) = 0$) coincides with that described by (28) if we set $\beta_2' \leftarrow 0$, $\nu(t) \leftarrow \gamma_{12}^I I_1$, $\alpha_2 \leftarrow \left(\delta_{21}^I + \alpha_2\right)$. Then we can immediately write down a solution for the PGF

$$G(z,t) = \exp\left\{\gamma_{12}^I (z-1) \int_0^t I_1(t')\, e^{-\left(\delta_{21}^I + \alpha_2\right)(t'-t)} \mathrm{d}t'\right\}$$

and the first moment

$$\bar{I}_{12} = \gamma_{12}^I \int_0^t \bar{I}_1(t')\, e^{-(\delta_{21}^I + \alpha_2)(t-t')} \mathrm{d}t'. \tag{45}$$

Flux process ν_{21} is more complicated and can be described by the following MC

Process	Rate
$S_{21} \to S_{21} + 1$	$\gamma_{21}^S N_2$
$S_{21} \to S_{21} - 1$	$\delta_{12}^S S_{21}$
$I_{21} \to I_{21} + 1, S_{21} \to S_{21} - 1$	$\beta_1 I_1 S_{21}$
$I_{21} \to I_{21} - 1$	$\delta_{12}^I I_{21}$

(46)

with the initial conditions $S_{21}(0) = \varepsilon_{21}^S N_2$, $I_{21}(0) = 0$. If we split the third event into two independent events $I_{21} \to I_{21} + 1$ and $S_{21} \to S_{21} - 1$ with the same rate, we can split MC (46) into two MCs. The first MC describes migration of host susceptible individuals from node 2 to node 1 and their possible removal due to contamination:

Process	Rate
$S_{21} \to S_{21} + 1$	$\gamma_{21}^S N_2$
$S_{21} \to S_{21} - 1$	$\left(\delta_{12}^S + \beta_1 I_1\right) S_{21}$

(47)

It is independent of the second MC with the rates

Process	Rate
$I_{21} \to I_{21} + 1$	$\beta_1 I_1 S_{21}$
$I_{21} \to I_{21} - 1$	$\left(\delta_{12}^I + \alpha_1\right) I_{21}$

(48)

which describes migration of susceptibles to a neighbor node, their contamination there and return to the host node as infected species.

We start with the first MC: see (47). In accordance with (19) it has the binomial initial distribution:

$$P_k(0) = \binom{N_2}{k} \left(\varepsilon_{21}^S\right)^k \left(1 - \varepsilon_{21}^S\right)^{N_2 - k}. \tag{49}$$

The probabilities $P_k(t) = \mathbb{P}(S_{21}(t) = k)$ of k guest susceptibles S_{21} at instant t satisfy Kolmogorov's equations for MC (28)

$$\tfrac{\mathrm{d}}{\mathrm{d}t} P_k = \nu \left(P_{k-1} - P_k\right) + \alpha \left[(\lceil k+1 \rceil_0^{N_2}) P_{k+1} - k P_k \right]. \tag{50}$$

where $\nu = \gamma_{21}^S N_2$, $\alpha = \left(\delta_{12}^S + \beta_1 I_1\right)$. System (50) implies the following PDE for MGF $G(z,t) = \sum_{k=0}^{\infty} z^k P_k(t)$

$$G_t = (z-1)\left[-\alpha(t) G_z + \nu G\right]. \tag{51}$$

The initial condition is

$$G(z,0) = \sum_{k=0}^{N} z^k \binom{N}{k} \varepsilon^k (1-\varepsilon)^{N-k} = (1 - \varepsilon + \varepsilon z)^N. \tag{52}$$

The initial value problem (51)–(52) admits the explicit solution

$$G(z,t) = \left[1 + \varepsilon(z-1)\phi(t)\right]^N \exp\left\{ \nu(z-1)\phi(t) \int_0^t \frac{\mathrm{d}t'}{\phi(t')} \right\} \tag{53}$$

where $\phi(t) = \exp\left\{-\int_0^t \alpha(t')\mathrm{d}t'\right\}$. From here we have

$$\mathbb{E}S_{21}(t) = G_z(1,t) = N_2\left[\varepsilon_{21}^S + \gamma_{21}^S \int_0^t \mathrm{d}t'/\phi(t')\right]\phi(t). \tag{54}$$

In analogy with processes (28) and (44) we can immediately write for process (48)

$$\bar{I}_{21} = \beta_1 \int_0^t e^{-\left(\delta_{12}^I+\alpha_2\right)(t-t')}\mathbb{E}\left[I_1\left(t'\right)S_{21}(t')\right]\mathrm{d}t'. \tag{55}$$

Neglecting the mutual dependence of processes $S_{21}(t)$ and $I_1(t)$ we approximate

$$\mathbb{E}\left[S_{21}(t)I_1(t)\right] \approx \mathbb{E}S_{21}(t)\bar{I}_1(t). \tag{56}$$

Thus the first moment $\bar{I}_2$ is calculated via (36) where $\bar{\nu}$ is given by (29) in which $\bar{I}_{12}$ is given by (45) and $\bar{I}_{21}$ is given by (55)–(56), in turn $\mathbb{E}S_{21}$ is calculated by (54) in which $\alpha(t) = \delta_{12}^S + \beta_1\bar{I}_1(t)$. The second moment is calculated via sum of convolutions (43) of $\bar{I}_{12}$ and $\bar{I}_{21}$.

Below we show numerically that it is a satisfactory approximation for our applications.

4.3. The second stage

Remember that equations (35), (41), (42), (43), (45), (55), (56) are valid at the contamination stage only ($S_2 \approx N_2$). These relationships allow us to calculate the first and second moments for the number of infectives without modelling the random process directly. To evaluate the moments at the developed outbreak we use the same approach as in [2]: by approximating the outbreak via the mean field solution for a single SIR node with random initial conditions.

For this aim, we define the intermediate time t_* such that the number of infective is large enough to use the mean field solution but the number of infective still slightly deviate from N_2: $\hat{I}_2(t_*) \gg 1$ and $N_2 - \hat{S}_2 \ll N_2$.

Then we generate L times a random number X lognormally distributed (to guarantee the positiveness) with mean $\bar{I}_2(t_*)$ and variance $\mathrm{var}(I_2(t_*))$ and integrate the classical SIR equations: $\frac{\mathrm{d}}{\mathrm{d}t}\hat{S}_2 = -\beta_2 \hat{S}_2 \hat{I}_2$, $\frac{\mathrm{d}}{\mathrm{d}t}\hat{I}_2 = (\beta_2 \hat{S}_2 - \alpha_2)\hat{I}_2$ with initial condition $\hat{I}_2(t_*) = X$,

$$\hat{S}_2(t_*) = -W_{-1}\left[-\beta_2' N_2 \exp\left\{\beta_2'(X - N_2)\right\}\right]/\beta_2'$$

where $W_k[\cdot]$ is the kth branch of the Lambert function [19].

Let us emphasize that in the classical SIR model, the numbers of susceptives and infectives are related as $I = N - S + \ln\left[S/(N - I_0)\right]/\beta'$ where $\beta' = \beta N$ (cf. [6]). Resolving this relation with respect to S we can write

$$S = -W_k\left[-\beta'(N - I_0)\exp\left\{\beta'(I - N)\right\}\right]/\beta'$$

where $k = -1$ for the growing part and $k = 0$ for the decaying part of the outbreak. If the outbreak is triggered by a infinitesimal number of infectives we can set $S = -W_k\left[-\beta' N \exp\left\{\beta'(I - N)\right\}\right]/\beta'$.

Also note that it is natural to approximate the solution to a standard SIR model by the limiting solution ($I_0/N \to 0$) introduced in [3]. The limiting solution is independent of the initial condition, therefore it is not necessity to integrate the ODEs L times, but only once.

Thus the proposed two-stage model of a coupled stochastic epidemic centers allows us to calculate its first moments much faster than the direct simulation summarized in Table 1.

4.4. Comparison with numerical simulation

To show the accuracy of the proposed model we compare the solutions obtained by the different approaches. Again the basic model of Section 3 is used: $N_1 = N_2 = 10\text{k}$, $\beta'_{1,2} = 4$, $\alpha_{1,2} = 1$, $\varepsilon^{S,I}_{1,2} = 0.01$, $\tau^{S,I}_{1,2} = 5$, $I_0/N_1 = 0.01$ but also model with the smaller population $N_1 = N_2 = 2\text{k}$. We compare (i) the full stochastic model described in Table 1 which we regard as a benchmark; (ii) the SIC approximate stochastic model where only flux of infectives from node 1 to node 2 is accounted, it is described in Table 3; (iii) the two-stage semi-random model proposed in this section above.

In the two-stage model we take time $t_* = 2.0$ for transition from a contamination stochastic stage to the mean-field stage with random initial condition. The expected number of infectives in node 2 at time $t = 2.0$ is 100 which is large enough and at the same time much smaller than the node population. We take $L = 10^4$ for number of realization in the second stage to evaluate the moments.

In the SIC approximation, the stochastic model presented in Table 3 comprises four consequently independent MCs. Processes 1 and 2 represent an independent outbreak in node 1 (26). Processes 3 and 4 represent migration of its infectives to node 2 (44). Processes 5 and 6 represent migration of host susceptives from node 2 to node 1 and their possible removal due to contamination; they are analogous to MC (47) with N_2 substituted by S_2 to be valid for all the stages. Similarly, processes 7 and 8 represent contamination of S_{21} in the first node and migration of appeared infectives I_{21} to their host node (48). Finally processes 9–10 represent the outbreak in node 2 ; they are analogous to a MC with an additional flux (28), having an accurate account

Table 3: MC for two interacting centers in the SIC approximation

i	Process $\#i$	Rate
1	$S_1 \to S_1 - 1$ $I_1 \to I_1 + 1$	$\beta_1 I_1 S_1$
2	$I_1 \to I_1 - 1$	$\alpha_1 I_1$
3	$I_{12} \to I_{12} + 1$	$\gamma_{12}^I I_1$
4	$I_{12} \to I_{12} - 1$	$\delta_{21}^I I_{12}$
5	$S_{21} \to S_{21} + 1$	$\gamma_{21}^S S_2$
6	$S_{21} \to S_{21} - 1$	$\left(\delta_{12}^S + \beta_1 I_1\right) S_{21}$
7	$I_{21} \to I_{21} + 1$	$\beta_1 I_1 S_{21}$
8	$I_{21} \to I_{21} - 1$	$\alpha_1 I_{21}$
9	$S_2 \to S_2 - 1$ $I_2 \to I_2 + 1$	$\beta_2 (I_2 + I_{12}) S_2 + \delta_{12}^I I_{21}$
10	$I_2 \to I_2 - 1$	$\alpha_2 I_2$

of the number of succeptives S_2 at all the stages.

The results of the computations are presented in Figures 10 and 11. Here, the bold lines indicate the full stochastic model, the thin solid lines indicate the SIC approximated model, the line with dots indicate the two-stage semi-random model. Also the mean-field solution is presented, and indicated by dashed lines.

Evidently, the proposed two-stage semi-random model gives quite a satisfactory approximation for the first two moments of the total number of infectives in node 2 if the population is 10k but only qualitative similarity for the smaller population. This justifies the used simplifications for rather moderate populated sites, but for the sites with population 2k and smaller

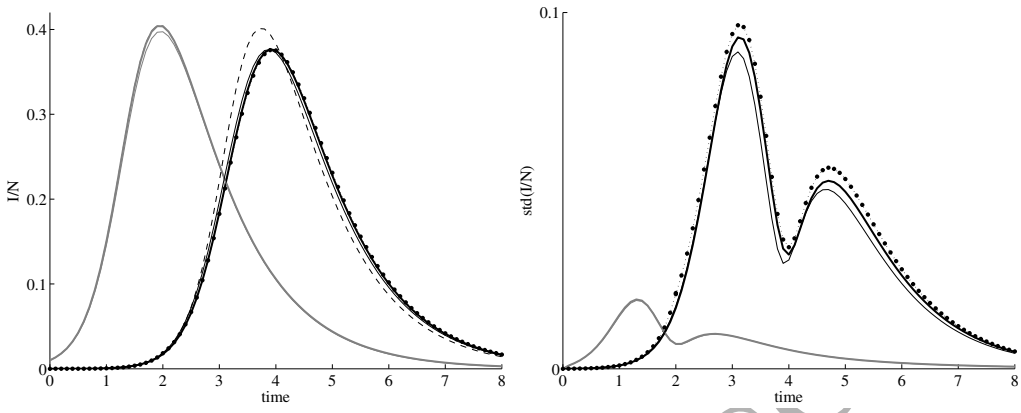

Figure 10: Comparison of different approximations for the mean value of infectives (left) and its standard deviation (right) for the basic model: populations $N_1 = N_2 = 10$k, migration parameters $\varepsilon = 0.01, \tau = 5$, initial share of infectives $I_0/N_1 = 0.01$, number of realisations in the simulations $L = 10^4$. Bold line – full stochastic model (Table 1), thin line – approximate stochastic model (Table 2), line with dots – the proposed two-stage semi-random model, dashed line – the mean field solution.

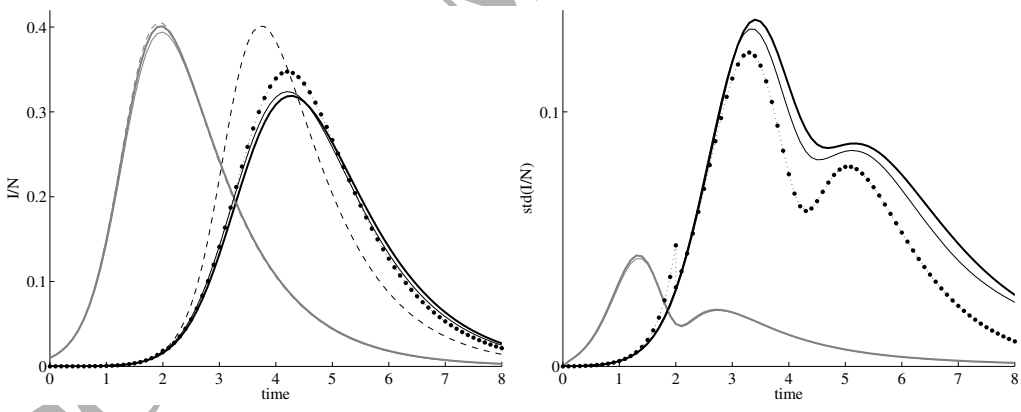

Figure 11: The same as in Figure 10 but for $N_1 = N_2 = 2$k.

more sophisticated models should be developed. In would be interesting to investigate the convergence of estimates for mean value of infectives obtained

from the full and two-stage models. This can be a subject of consequent works.

5. Discussion

We present a stochastic network of SIR models, coupled by random migration fluxes as described in terms of Markov chains. In the absence of infectives, a pure migration of individuals is well described as a simple MC: if disturbed, the system returns to a dynamic equilibrium exponentially fast, in a manner that resembles a diffusion process in physics.

In the mean-field (hydrodynamic) limit, the MC converges to a non-standard network SIR model: the host and guest species are treated separately in the corresponding ODEs (4)–(7).

A traditional approach to account for the coupling between the nodes is to include transport terms into the equations (cf. [6, 20]):

$$\begin{aligned} \tfrac{\mathrm{d}}{\mathrm{d}t}S_n &= -\beta_n S_n I_n + \chi^S_{mn} S_m \\ \tfrac{\mathrm{d}}{\mathrm{d}t}I_n &= \beta_n S_n I_n - \alpha_n I_n + \chi^I_{mn} I_m. \end{aligned} \tag{57}$$

Simple analysis shows that pure migration in the equations of type (57) possesses inappropriate exponentially growing solutions [12]. This instability is often ignored as it can be hidden in the background of the outbreak and not be observable in certain epidemic model scenarios.

The model proposed in [21, 22]

$$\begin{aligned} \tfrac{\mathrm{d}}{\mathrm{d}t}S_n &= -\beta_n S_n I_n + \chi^S_{mn} S_m - \chi^S_{nm} S_n \\ \tfrac{\mathrm{d}}{\mathrm{d}t}I_n &= \beta_n S_n I_n - \alpha_n I_n + \chi^I_{mn} I_m - \chi^I_{nm} I_n \end{aligned}$$

gives more stable pure migration. However, a simple analysis shows that in this model we obtain the fully mixed population in all the nodes [12] ($\varepsilon = 0.5$

in our terms). Thus the dynamics of this model seems to be more realistic but nevertheless does not satisfy an intuitive interpretation of the equilibrium of the migration process.

Both above models are characterized by only one parameter describing migration of a given species. This makes it impossible to tune the model to obtain the realistic migration process in the absence of the outbreak.

In our earlier work [4] a migration model is introduced without splitting species into host and guest, with two migration parameters: ε and τ describing migration process of a given species. But the model proposed in [4] also does not give a completely satisfactory solution for pure migration in the case of different migration times: τ_{12}^S and τ_{21}^S as shown in [12].

Though the effect of the more correct account of migration can be very small for some combination of the epidemic and migration parameters, it can become essential when parameters of the model vary in a wide range.

In the present work, three different techniques for the model under consideration are compared: a MC describing the number of individuals from all categories in both centers, its hydrodynamical limit in the form of a system of dynamic equations and a simple description of contamination stage at the node 2 as an isolated center with an inflow of infectives neglecting the backward migration. In our approach, the random evolution on the contamination stage either in its full or simplified form is coupled with the dynamical description on the stage of saturation. This makes the problem computationally feasible. Our intention is to apply this technique to a network of interacting population centers in future work. Note that the direct simulation of the network is extremely expensive in terms of the CPU time

compared with integration of the dynamical equations. The computational time may be considerably reduced if the simulation is required during a relatively short contamination periods only.

The spatial structure of population is a key element in the understanding of the large-scale spread of epidemics. The arrival of an infection and its epidemic evolution are determined by the mobility processes among subpopulations. The account of the movement of individuals has generated a wealth of models and results (see [23, 24, 25, 26, 27, 28] and references therein). In a number of papers, the evolution of an epidemic is described by a deterministic reaction-diffusion equation (see [29, 30] and references therein). Among important issue in the dynamics of directly transmitted diseases is the relationship between infection rate and host density. Another important aspect is the different dynamics of host and guest species on the epidemic speed. For a purely deterministic model, the account of different dynamics of host and guest species on the epidemic speed was studied in [12]. The simplifying assumptions make the analysis tractable but may not adequately reflect reality. It seems that a network of stochastically interacting centers of the type discussed above may provide more realistic but still tractable setting.

In the next paper we intend to derive the travelling wave characteristic equation (cf. [3, 4, 12]) and explore analytically and numerically the dependence of the mean epidemic speed and its standard deviation on the network parameters.

Acknowledgment

The financial support within the framework of a subsidy granted to the National Research University Higher School of Economics for the implementation of the Global Competitiveness Programme is acknowledged.

References

[1] S. M. Ross, First Course of Probability, Prentice Hall, NJ, 2008.

[2] I. Sazonov, M. Kelbert, M. B. Gravenor, A two-stage model for the sir outbreak: Accounting for the discrete and stochastic nature of the epidemic at the initial contamination stage, Mathematical Biosciences 234 (2) (2011) 108–117. doi:10.1016/j.mbs.2011.09.002.

[3] I. Sazonov, M. Kelbert, M. B. Gravenor, The speed of epidemic waves in a one-dimensional lattice of SIR models, Mathematical Modeling of Natural Phenomena 3 (4) (2008) 28–47.

[4] I. Sazonov, M. Kelbert, M. B. Gravenor, Travelling waves in a lattice of SIR nodes in approximation of weak coupling, Mathematical Biology and Medicine 28 (2) (2011) 165–183. doi:10.1093/imammb/dqq016.

[5] A. H. Nayfeh, Perturbation Methods, John Wiley & Sons, New York, London, etc., 1973.

[6] D. J. Daley, J. Gani, Epidemic Modeling, Cambridge University Press, Cambridge, 1999.

[7] F. Ball, D. Mollison, G. Scalia-Tomba, Epidemics with two levels of mixing, The Annals of Applied Probability 7 (1) (1997) 46–89.

[8] H. Andersson, T. Britton, Stochastic Epidemic Models and Their Statistical Analysis, Springer-Verlag, New York, 2000.

[9] M. J. Keeling, J. V. Ross, On methods for studying stochastic disease dynamics, Journal of The Royal Society Interface 5 (19) (2008) 171–181.

[10] O. Diekmann, H. Heesterbeek, T. Britton, Mathematical Tools for Understanding Infectious Disease Dynamics, Princeton University Press, Princeton, 2012.

[11] B. Meerson, P. V. Sasorov, WKB theory of epidemic fade-out in stochastic population, Physical Review E 80 (4) (2009) 1–4. doi:10.1103/PhysRevE.80.041130.

[12] I. Sazonov, M. Kelbert, A new view on migration processes between sir centra: an account of the different dynamics of host and guest, arXiv: 1401.6830v1 [q-bio. PE].

[13] T. G. Kurtz, Solutions of ordinary differential equations as limits of pure jump Markov processes, Journal of Applied Probability 7 (1970) 49–58.

[14] A. D. Barbour, Equilibrium distributions Markov population processes, Advances in Applied Probability 12 (3) (1980) 591–614.

[15] D. E. Mollison, Epidemic Models: Their Structure and Relation to Data, Cambridge University Press, Cambridge, 1995.

[16] J. D. Murray, Mathematical Biology, Springer, London, 1993.

[17] R. W. R. Darling, Fluid limits of pure jump Markov processes: a practical guide, Tech. rep., National Security Agency, P. O. Box 535, Annapolis Junction, MD 20701 (July 2002).

[18] Y. Suhov, M. Kelbert, Probability and Statistics by Example. Vol.II, Markov Chains: A Primer in Random Processes and their Applications., Cambridge University Press, Cambridge, 2008.

[19] R. M. Corless, G. H. Gonnet, D. E. G. Hare, D. J. Jeffrey, D. E. Knuth, On the Lambert W function, Advances in Computational Mathematics 5 (1996) 329–359.

[20] W. Wang, X. Zhao, Threshold of disease transmission in a patch environment, Mathematical Biosciences 190 (1) (2004) 97–112.

[21] W. Wang, G. Mulone, Threshold of disease transmission in a patch environment, Journal of Mathematical Analysis and Applications 285 (1) (2003) 321–335.

[22] J. Arino, J. Davis, D. Hartley, R. Jordan, J. Miller, P. van den Driessche, A multi-species epidemic model with spatial dynamics, Mathematical Medicine and Biology 22 (2) (2005) 129–142.

[23] D. Mollison, Dependence of epidemic and population velocities on basic parameters, Mathematical Biosciences 107 (1991) 255–287.

[24] B. Bolker, B. Grenfell, Space, persistence and dynamics of measles epidemics, Philosophical Transactions of The Royal Society B Biological Sciences 348 (1325) (1995) 309–320. doi:10.1098/rstb.1995.0070.

[25] B. T. Grenfell, A. Kleczkowski, C. A. Gilligan, B. M. Bolker, Spatial heterogeneity, nonlinear dynamics and chaos in infectious diseases, Statistical Methods in Medical Research 4 (2) (1995) 160–183. doi:110.1038/414716a.

[26] J. Arino, R. Jordan, P. van den Driessche, Quarantine in a multi-species epidemic model with spatial dynamics, Mathematical Bioscience 206 (2007) 46–60.

[27] S. Bansal, B. T. Grenfell, L. A. Meyers, Large-scale spatial-transmission models of infectious disease, Science 316 (1325) (2007) 1298–1301. doi:10.1126/science.1134695.

[28] J. Burton, L. Billings, D. A. Cummings, I. B. Schwartz, Disease persistence in epidemiological models: the interplay between vaccination and migration, Mathematical Bioscience 239 (1) (2012) 91–96. doi:10.1016/j.mbs.2012.05.003.

[29] V. Colizza, A. Vespignani, Invasion threshold in heterogeneous metapopulation networks, Physical Review Letters 99 (2007) 148701. doi:10.1103/PhysRevLett.99.148701.

[30] B. T. Grenfell, B. T. Bjørnstad, J. Kappey, Travelling waves and spatial hierarchies in measles epidemics, Nature 4141 (2001) 716–723. doi:110.1038/414716a.

[31] M. Kelbert, I. Manolopoulou, I. Sazonov, Y. M. Suhov, Large deviations for a model of excess of loss re-insurance, Markov Processes and Related Fields 13 (1) (2007) 137–158.

[32] A. Muller, D. Stoyan, Comparison Methods for Stochastic Models and Risks, Wiley, N.Y., 2002.

Appendix A. Sketch of the proof to Proposition 1.

First, the mean values of the Markov chain (MC) converges to the solution of initial value problem (4)–(9) by the LLN. The phenomenological sketch is given Section 1, and the rigorous proof is analogous to that presented in [13, 17, 31].

We also must establish the convergence in probability. For definiteness consider $I_2(t)$ and apply Chebyshev's inequality for any $\epsilon > 0$

$$\mathbb{P}\Big(\Big|\frac{I_2(t)}{\Lambda} - \hat{I}_2(t)\Big| > \epsilon\Big) \le \frac{\mathrm{var}\,[I_2(t)]}{\Lambda^2\epsilon^2}.$$

Recall that Λ is the population scaling parameter (see Section 1). So, it is enough to check that

$$\mathrm{var}\,[I_2(t)] = O(\Lambda), \qquad \Lambda \to \infty. \tag{A.1}$$

This fact is demonstrated numerically in Section 3 (see Figure 3). Actually, we see that the normalized standard deviation decays as $N^{-1/2}$, or equivalently, the non-normalized standard deviation grows as $N^{1/2}$ (i.e., as $\Lambda^{1/2}$), that implies (A.1).

The rigorous argument runs as follows. Consider the processes in Table 1 which cause the change in number of infectives in node 2 and outline the fluxes of infectives. These processes are

#	Event	Rate
9,16	$I_2 \to I_2 + 1$	$\beta_2 I_2 S_2 + \underline{\beta_2 I_{12} S_2 + \delta^I_{12} I_{21}}$
11,14	$I_2 \to I_2 - 1$	$\alpha_1 I_2 + \underline{\gamma^I_{21} I_2}$

(A.2)

Here the flux terms are underlined, the remaining terms describe the MC based stochastic SIR model [6, 2]. So the real flux can be defined as

$$\nu(t) = \beta_2 I_{12} S_2 + \delta^I_{12} I_{21} - \gamma^I_{21} I_2.$$

We construct the process $\tilde{I}_2$

Event	Rate
$\tilde{I}_2 \to \tilde{I}_2 + 1$	$\beta'_2 \tilde{I}_2 + \tilde{\nu}$
$\tilde{I}_2 \to \tilde{I}_2 - 1$	$\alpha_1 \tilde{I}_2$

(A.3)

with the majorized constant flux

$$\tilde{\nu} = \beta'_2 N_1 + \delta^I_{12} N_2 \geq \nu(t).$$

Remind that $\beta'_2 = \beta_2 N_2$ is a constant when $\Lambda \to \infty$.

For this process we have a stochastic SI model (considered in [13]) with the constant Poisson flux $\tilde{\nu}$. This problem is solved in Section 4 and it is shown that its variance grows as $O(\Lambda)$.

Next, we establish the second order stochastic domination (see [32] for details) of process $I_2(t)$ by $\tilde{I}_2(t)$. In fact the following inequality holds for all $x, t \geq 0$ (cf. [32])

$$\int_0^x \mathbb{P}\big(I_2(t) \geq u\big)\mathrm{d}u \leq \int_0^x \mathbb{P}\big(\tilde{I}_2(t) \geq u\big)\mathrm{d}u.$$

The second order stochastic domination means that for any convex function $\Psi(\cdot)$ we have the inequality for all $t \geq 0$

$$\mathbb{E}[\Psi(I_2(t))] \leq \mathbb{E}[\Psi(\tilde{I}_2(t))],$$

$\tilde{I}_2(t)$ is the number of susceptible in the tractable model described by (A.3). In our case $\Psi(X) = (X - \mathbb{E}X)^2$. This implies the inequality $\text{var}\,[I_2(t)] \leq \text{var}\left[\tilde{I}_2(t)\right]$. $\square$